Noise-induced transport of two coupled particles

Stefan Klumpp,* Andreas Mielke,† and Christian Wald‡
Institut für Theoretische Physik der Universität Heidelberg, Philosophenweg 19, 69120 Heidelberg, Germany
(Received 3 April 2000; revised manuscript received 17 August 2000; published 27 February 2001)

We study the motion of two harmonically coupled particles in a sawtooth potential. The particles are subject to temporally correlated multiplicative noise. The stationary current is calculated in an expansion about the limit of rigid coupling. For two coupled particles a driving mechanism occurs which is different from the one occurring in the case of a single particle. In particular this mechanism does not need diffusion. Depending on the equilibrium distance of the particles and the coupling constant, a current reversal occurs. Possible relevance as a model for motor proteins is discussed.

DOI: 10.1103/PhysRevE.63.031914 PACS number(s): 87.16.Nn, 05.40.−a

I. INTRODUCTION AND MAIN RESULTS

For some years the problem of noise-induced transport has attracted much interest in theoretical (for a review, see Refs. [1,2] and references therein) as well as experimental physics [3,4]. From a physical point of view the motivation to study models for noise-induced transport is to study the conditions under which noise out of equilibrium can induce directed motion, even if the average force is zero. In general, to obtain directed motion two conditions must be fulfilled: (1) The periodic potential must have no inversion symmetry. (2) Detailed balance has to be broken. In the Brownian regime, the second condition can be satisfied by the use of colored noise, i.e., noise correlated in time [5]. Mainly two types of models are studied: A particle in a periodic potential subject to a stochastic force (additive colored noise, rocking ratchet [5]) and a particle in a fluctuating periodic potential (multiplicative colored noise, flashing ratchet [6,7]).

Besides this purely physical motivation, the theoretical study of noise-induced transport has been stimulated by experiments on motor proteins such as kinesin or dynein. Motor proteins move cell organelles along the cytosceleton. Their motion is random, but directed on average [8,9]. Energy is provided by adenosine triphosphate (ATP) hydrolysis. ATP coupling to a motor protein induces a series of conformational changes. These are modeled by transitions between different states, in which the protein is subject to different potentials. Alternatively one can consider a protein moving in a fluctuating potential. The potential models the interaction of the motor protein with the filaments of the cytosceleton. It is periodic and has no inversion symmetry because of the polar structure of the filament. As ATP hydrolysis drives the motor system out of detailed balance, conditions for transport are satisfied. Models for noise-induced transport can qualitatively explain some properties of motor proteins.

In this paper we discuss a model that is inspired by the structural properties of motor proteins. Processive motor proteins usually consist of two spherical heads, joined by a neck region, and a tail, at which the cargo is attached. Each head can couple to the filaments of the cytosceleton and hydrolyze ATP.

Several authors studied the motion of two coupled particles modeling the two heads of a motor protein [10–13]. Both types of ratchet models have been studied: Ajdari considered the case of multiplicative potential fluctuations in the case of weak coupling [10], whereas Derényi and Vicsek discussed the case of stochastic forces [11]. The models of Peskin and Oster [12] and Duke and Leibler [13] rely on a different mechanism based on transition times depending on strain of the heads.

In this paper we present results for a model with two particles moving in a fluctuating periodic potential and coupling independently to thermal and colored noise (Fig. 1). The two particles are harmonically coupled. In contrast to Ref. [10] we consider the case of strong coupling.

The paper is organized as follows: In Sec. II we present the model, and introduce the Fokker-Planck equation. In Sec. III the general method of solution is explained: We solve the stationary Fokker-Planck equation in an expansion about the case of rigid coupling, and derive a set of equations of the type of a Fokker-Planck equation for a single particle. These are solved using methods described in Ref. [14] for the case of a piecewise linear potential (Sec. IV). Some mathematical details are presented in the Appendixes. In Sec. V we present numerical results for special stochastic processes, and discuss the current as a function of the correlation time of the noise and the equilibrium distance of the two particles. There are current reversals not only of the current as a function of the correlation time, but also as a function of the equilibrium distance. In addition, for two coupled particles there is a driving mechanism that does not need diffusion: If the equilibrium distance of the particles is larger than the short section of the sawtooth potential, one particle can be pushed or

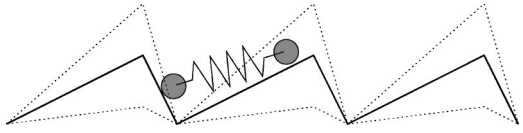

FIG. 1. The model: Two coupled particles in a sawtooth potential, which fluctuates independently for each particle

*Present address: Max-Planck-Institut für Kolloid- und Grenzflächenforschung, 14424 Potsdam, Germany.
Email address: klumpp@mpikg-golm.mpg.de
†Email address: mielke@tphys.uni-heidelberg.de
‡Email address: wald@tphys.uni-heidelberg.de

pulled forward by the other. In Appendix B we compare the results with those for a model with additive stochastic forces instead of multiplicative potential fluctuations. In this case, the model with two rigidly coupled particles can be reduced to a one-particle model. Finally we summarize the results and discuss possible relevance of the model for motor proteins (Sec. VI).

Open questions concern the current as a function of the coupling constant. In the case of weak coupling there is a slightly different driving mechanism [10]. To study the transition from strong to weak coupling, other methods have to be used, especially computer simulations. We show some results of the simulations in Sec. V. These results indicate that the order of magnitude of the current does not change when the coupling constant is varied. But in some cases, depending on the other parameters of the model, we observe a current reversal. On the other hand, simulations allow to study refined models for motor proteins. The present model imitates only some (but perhaps important) aspects of motor proteins.

II. MODEL WITH TWO COUPLED PARTICLES

We consider two harmonically coupled particles moving in a periodic potential V. The particles are subject to thermal noise ξ_i at temperature T, and multiplicative nonwhite potential fluctuations z_i ($i=1$ and 2). z_1 and z_2 are stochastic processes of the same type correlated in time with correlation time τ, but independent of each other:

$$\langle \xi_i(t)\rangle = 0, \quad \langle \xi_i(t)\xi_j(t')\rangle = \delta_{i,j}\delta(t-t'), \tag{1}$$

$$\langle z_i(t)z_j(t')\rangle - \langle z_i(t)\rangle\langle z_j(t')\rangle = \gamma_{0,1}^2\delta_{i,j}e^{-|t-t'|/\tau}. \tag{2}$$

In the overdamped regime we have the Langevin equations

$$\dot{x}_1 = f(x_1)z_1(t) - \tfrac{1}{2}\kappa(x_1-x_2-l) + \sqrt{2T}\xi_1, \tag{3}$$

$$\dot{x}_2 = f(x_2)z_2(t) + \tfrac{1}{2}\kappa(x_1-x_2-l) + \sqrt{2T}\xi_2, \tag{4}$$

where $f(x_i) = -\partial V/\partial x_i$. κ is the coupling constant, and l is the equilibrium distance of the particles. Here we have set the friction constant to one by rescaling the time variable. We introduce center of mass and relative coordinates $x = (x_1+x_2)/2$ and $y = (x_1-x_2-l)/2$. The Langevin equations are equivalent to a Fokker-Planck equation for the joint probability density $\rho(x,y,z_1,z_2,t)$,

$$\begin{aligned} -\frac{\partial}{\partial x}\left[\frac{z_1}{2}f\left(x+\frac{l}{2}+y\right)+\frac{z_2}{2}f\left(x-\frac{l}{2}-y\right)-\frac{T}{2}\frac{\partial}{\partial x}\right]\rho \\ -\frac{\partial}{\partial y}\left[\frac{z_1}{2}f\left(x+\frac{l}{2}+y\right)-\frac{z_2}{2}f\left(x-\frac{l}{2}-y\right) \right. \\ \left. -\kappa y-\frac{T}{2}\frac{\partial}{\partial y}\right]\rho + M_{z_1}\rho + M_{z_2}\rho = \frac{\partial \rho}{\partial t}, \end{aligned} \tag{5}$$

where we have assumed that z_i are Markov processes with generators M_{z_i}. As we are only interested in the stationary solution, we let $\frac{\partial \rho}{\partial t} = 0$. By averaging the left hand side of the Fokker-Planck equation over z_1, z_2, and y, we obtain the stationary current

$$\begin{aligned} J = \int_{-\infty}^{\infty} dy \int dz_1 \int dz_2 \left[\frac{z_1}{2}f\left(x+\frac{l}{2}+y\right)\right. \\ \left. +\frac{z_2}{2}f\left(x-\frac{l}{2}-y\right)-\frac{T}{2}\frac{\partial}{\partial x}\right]\rho. \end{aligned} \tag{6}$$

III. EXPANSION ABOUT RIGID COUPLING

We solve the stationary Fokker-Planck equation in an expansion about the limit of rigid coupling. We introduce a new coordinate $\tilde{y} = \sqrt{\kappa}y$ and expand the force terms in Eq. (5) in powers of $1\sqrt{\kappa}$. With the ansatz

$$\rho = \rho_0 + \frac{1}{\sqrt{\kappa}}\rho_{1/2} + \frac{1}{\kappa}\rho_1 + \frac{1}{\kappa^{3/2}}\rho_{3/2} + \cdots, \tag{7}$$

we obtain a set of equations for the powers of $\sqrt{\kappa}$. From these equations we can calculate the $\tilde{y}$ dependence of ρ_s ($s = 0, \frac{1}{2}, 1$), which is given in Appendix A1, and by averaging over $\tilde{y}$ we obtain equations for the averaged functions

$$\overline{\rho_s}(x,z_1,z_2) = \int_{-\infty}^{\infty} d\tilde{y}\, \rho_s(x,\tilde{y},z_1,z_2), \tag{8}$$

that have a structure similar to the Fokker-Planck equation for one particle and thus can be solved using similar methods:

$$\begin{aligned} \frac{\partial}{\partial x}\left[\frac{z_1}{2}f\left(x+\frac{l}{2}\right)+\frac{z_2}{2}f\left(x-\frac{l}{2}\right)-\frac{T}{2}\frac{\partial}{\partial x}\right]\overline{\rho_0} \\ = M_{z_1}\overline{\rho_0} + M_{z_2}\overline{\rho_0}, \end{aligned} \tag{9}$$

$$\begin{aligned} \frac{\partial}{\partial x}\left[\frac{z_1}{2}f\left(x+\frac{l}{2}\right)+\frac{z_2}{2}f\left(x-\frac{l}{2}\right)-\frac{T}{2}\frac{\partial}{\partial x}\right]\overline{\rho_{1/2}} \\ = M_{z_1}\overline{\rho_{1/2}} + M_{z_2}\overline{\rho_{1/2}}, \end{aligned} \tag{10}$$

$$\begin{aligned} 0 = \frac{\partial}{\partial x}\left[\frac{z_1}{2}f\left(x+\frac{l}{2}\right)+\frac{z_2}{2}f\left(x-\frac{l}{2}\right)-\frac{T}{2}\frac{\partial}{\partial x}\right]\overline{\rho_1} \\ +2T\frac{\partial}{\partial x}\left[\frac{z_1}{4}f''\left(x+\frac{l}{2}\right)+\frac{z_2}{4}f\left(x-\frac{l}{2}\right)\right]\overline{\rho_0} \\ +\frac{\partial}{\partial x}\left\{\frac{z_1^2}{4}f\left(x+\frac{l}{2}\right)f'\left(x+\frac{l}{2}\right)+\frac{z_2^2}{4}f\left(x-\frac{l}{2}\right)f'\left(x-\frac{l}{2}\right)\right. \end{aligned}$$

$$-\frac{z_1 z_2}{4}\left[f\left(x+\frac{l}{2}\right)f'\left(x-\frac{l}{2}\right)+f\left(x-\frac{l}{2}\right)f'\left(x+\frac{l}{2}\right)\right]\Bigg\}\overline{\rho_0}$$
$$-(M_{z_1}+M_{z_2})\overline{\rho_1}. \tag{11}$$

The contributions to the current, in the corresponding order J_s $(s=0,\frac{1}{2},1)$, are obtained analogously to Eq. (6). In addition to these equations we have periodic boundary conditions $[\overline{\rho_s}(x+L)=\overline{\rho_s}(x)]$ and conditions for the normalization of the probability density:

$$\int_0^L dx \int dz_1 \int dz_2\, \overline{\rho_0}(x+L)=1, \tag{12}$$

$$\int_0^L dx \int dz_1 \int dz_2\, \overline{\rho_s}(x+L)=0, \quad s=\frac{1}{2} \text{ and } 1. \tag{13}$$

For M_{z_1} and M_{z_2} we take a class of processes with the properties:

$$M_{z_i}\phi_n(z_i)=-\lambda_n\phi_n(z_i), \tag{14}$$

$$\phi_0=q(z_i), \quad \lambda_0=0, \quad \lambda_n>0 (n>0), \tag{15}$$

$$z_i\phi_n(z_i)=\gamma_{n-1,n}\phi_{n-1}+\gamma_{n,n+1}\phi_{n+1}+\gamma_{n,n}\phi_n, \tag{16}$$

where $q(z_i)$ is the stationary distribution of z_i $[M_{z_i}q(z_i)=0]$ and $\gamma_{n-1,n}=\gamma_{n,n-1}$. The parameters $\gamma_{n-1,n}$ are related to the moments of the stationary distribution [14]. We expand ρ_s $(s=0,\frac{1}{2},1)$ in the eigenfunctions of the generators M_{z_1} and M_{z_2}. Using Eq. (16), we obtain recursion relations, that we solve for the case of a sawtooth potential.

IV. SOLUTION FOR A PIECEWISE LINEAR POTENTIAL

In this section we solve Eqs. (9)–(11) for the case of a sawtooth potential. The method of solution is similar to the one used in Ref. [14]. We consider the case of a sawtooth potential with the following properties of the force $f(x)$:

$$f(x)=\begin{cases} f_1: & 0<x\leqslant L_1 \\ f_2: & L_1<x\leqslant L, \end{cases} \tag{17}$$

with $f_1L_1+f_2L_2=0$ and $L_2=(L-L_1)$. We assume that $f_1<0$ and $f_2>0$. We define length and energy units by $L=1$ and $\Delta V=L_1|f_1|=1$. The only remaining parameter for the potential is the asymmetry $a=L_1/L_2$, which we assume to be >1. For the results presented in Sec. V, we have chosen $a=4$, corresponding to $L_1=0.8$, $f_1=-1.25$, and $f_2=5$. In these units a current of -1 corresponds to the velocity of a particle subject to the force f_1 in the case of maximal asymmetry.

We define effective forces $f^{(+)}$ and $f^{(-)}$ by

$$f^{(+)}=f\left(x+\frac{l}{2}\right), \quad f^{(-)}=f\left(x-\frac{l}{2}\right) \tag{18}$$

and consider the intervals $I_k=(x_{k-1},x_k)$, $k=1,\ldots K$, where both $f^{(+)}$ and $f^{(-)}$ are constant. K can be 2, 3, or 4, depending on the equilibrium distance l of the particles.

A. Order κ^0

Expanding ρ_0 in the eigenfunctions of the generators M_{z_1} and M_{z_2},

$$\rho_0(x,z_1,z_2)=p_{0,0}(x)q(z_1)q(z_2),$$
$$+\sum_{i,j}(-1)^{i+j}p'_{i,j}(x)\phi_i(z_1)\phi_j(z_2), \tag{19}$$

and using relation (16), from Eq. (9), we obtain a recursion relation for the coefficients $p_{i,j}(x)$. As it is somewhat lengthy, it is given in the Appendix. It is solved analogously to the case of a single particle. The method is described in detail in Ref. [14]. As for a piecewise linear potential the recursion relation is a set of linear differential equations with constant coefficients for each interval I_k, solutions can be found for $x\in I_k$. Then a linear combination of these solutions is determined by the periodic boundary conditions, normalization, and continuity of ρ_0.

For the sawtooth potential the solution is for $x\in I_k$,

$$p_{0,0}(x)=\sum_{r=1}^{2(N+1)^2-1} c_{r,k}a^{(r)}_{0,0,k}\alpha^{(r)}_k \exp(\alpha^{(r)}_k x)+b_{0,0,k}, \tag{20}$$

$$p_{i,j}(x)=\sum_{r=1}^{2(N+1)^2-1} c_{r,k}a^{(r)}_{i,j,k} \exp(\alpha^{(r)}_k x)+b_{i,j,k}, \tag{21}$$

where the second equation holds for $i+j\geqslant 1$. α_k and $a_{i,j,k}$ are the solutions of a generalized eigenvalue problem of the following type:

$$\boldsymbol{A}\boldsymbol{a_k}=\alpha_k B_k \boldsymbol{a_k}+\frac{T}{2}\alpha_k^2\boldsymbol{a_k}. \tag{22}$$

In contrast to Ref. [14] the matrices A and B here are not tridiagonal. The constants $b_{i,j,k}$ are zero except

$$b_{0,0,k}=\frac{J_0}{\frac{\gamma_{0,0}}{2}(f_k^{(+)})+(f_k^{(-)})} \tag{23}$$

$$b_{1,0,k}=\frac{\gamma_{0,1}}{2\lambda_1}f_k^{(+)}b_{0,0,k}, \quad b_{0,1,k}=\frac{\gamma_{0,1}}{2\lambda_1}f_k^{(-)}b_{0,0,k}. \tag{24}$$

The coefficients $c_{r,k}$ and the current J_0 are calculated using conditions for the continuity of $p_{i,j}$ $(i,j \geqslant 0)$ and $p'_{i,j}$ $(i+j>0)$, and the normalization of $p_{0,0}$.

B. Order κ^{-1}

In the order $\kappa^{-1/2}$ we have the same recursion relation, but the normalization condition [Eq. (12)] is replaced by Eq. (13). This leads to the result that both $\rho_{1/2}$ and $J_{1/2}$ vanish.

For the order κ^{-1} the method has to be extended because of the terms where ρ_0 and $\rho_{1/2}$ occur in Eq. (11). This somewhat technical procedure is explained in the Appendixes. As in the order κ^0 this leads to a generalized eigenvalue problem for each interval I_k, and a set of conditions of how to combine the solutions in these intervals.

V. RESULTS

The results presented in this section have been obtained by numerically solving the eigenvalue problems [Eq. (22)] and the system of linear equations obtained from conditions combining these solutions. The advantage of this method of solution is that numerical calculations can be performed quickly, and curves like the ones shown here are obtained within a few seconds. The results have been checked by computer simulations of the dynamics given by the Langevin equations (3) and (4). These simulations are also used to estimate the range of validity of the expansion about rigid coupling.

A. Results for the case of rigid coupling (order κ^0)

1. Dichotomous processes

We first consider the case of symmetric dichotomous processes: z_1 and z_2 vary only between two values z_a and z_b, $\gamma_{1,1}=\gamma_{0,0}=(z_a+z_b)/2$ and $\gamma_{0,1}=(z_a-z_b)/2$. In the case $l=0$ the effective potential is $[(z_1+z_2)/2]V(x)$; thus the results are the same as in the case of one particle in a fluctuating potential, where the stochastic process is a sum of two dichotomous processes. In particular we obtain a current reversal for large correlation time τ, if $z_a<0$ and $z_a+z_b>0$ (the solid line in Fig. 2). For small positive l the current reversal vanishes. This is shown in Fig. 3. Thus there is a reversal of the direction of motion as a function of the equilibrium distance l.

In the case $z_a=0$ and $z_b>0$, there is no current reversal, but Fig. 2 shows that the maximal current is very sensitive on l. For $l=0.5$ the current is about four times larger than for $l=0$. If we plot the current as a function of l, we can see that the current is nearly constant, as long as l is smaller than the short section L_2 of the sawtooth potential. If $l>L_2$, the current grows rapidly.

The reason for this behavior is that for $l>L_2$ there is another driving mechanism, which is fundamentally different from the one occurring in the case of a single particle. This driving mechanism is shown in Fig. 4 for the case $l=0.5$. When $z_1=z_2=z_b>0$ there are two equilibrium positions. One particle (A) is bound in a potential minimum, and because of the rigid coupling the other [B in Fig. 4(a) and B' in Fig. 4(b), respectively] is not able to move to a minimum. If the potential changes to zero for the particle in the minimum, the other particle can move to the next minimum and push or pull the first particle to the left. If the potential changes to zero for particle B or B', respectively, nothing happens, if the other particle is bound in the potential minimum. If the potential is zero for both particles, this driving mechanism stops working, but there is the possibility of diffusion as in the case of a single particle. This driving mechanism is similar to the one discussed in Ref. [10], which occurs in the case of weak coupling of two particles. In this case, when the potential changes to zero for one particle, it is pushed forward by the relaxation of the spring between the particles. In the case of a single particle similar driving occurs if there are also fluctuations of the position of the potential minimum [17]. In all these cases diffusion is not necessary for motion.

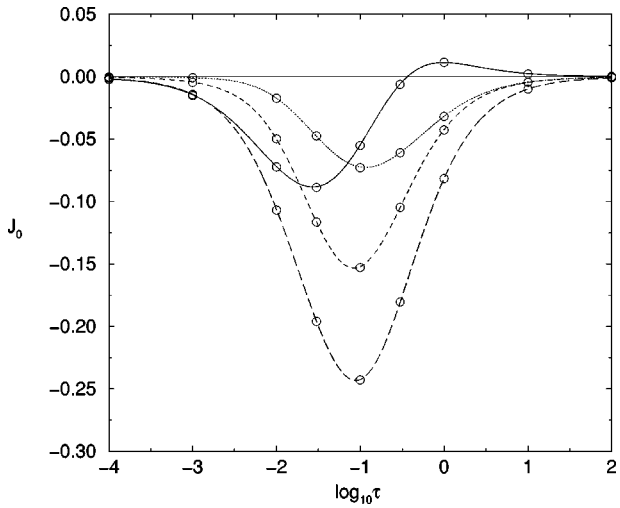

FIG. 2. Current J_0 as a function of τ for dichotomous processes: $z_a=-0.8, z_b=1.2, l=0$ (solid line) and $z_a=0, z_b=2$ for $l=0$,0.3, and 0.5 (dashed lines). The other parameters are $T=0.2$ and $a=4$. Here and in the following figures the symbols are results from simulations of the Langevin equation.

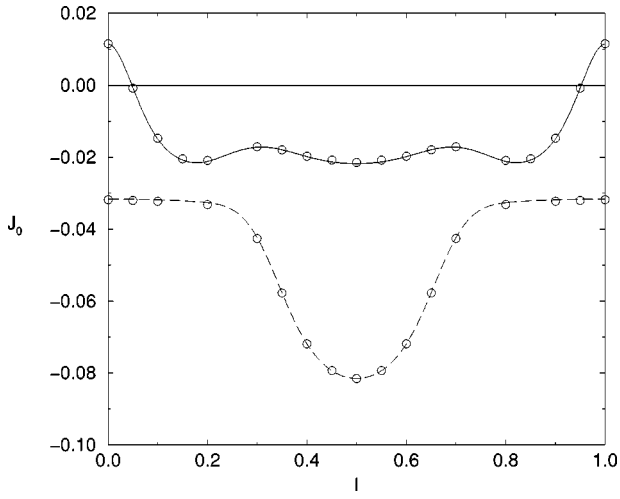

FIG. 3. Current J_0 as a function of l for dichotomous processes. The parameters are the same as in Fig. 2; $\tau=1$.

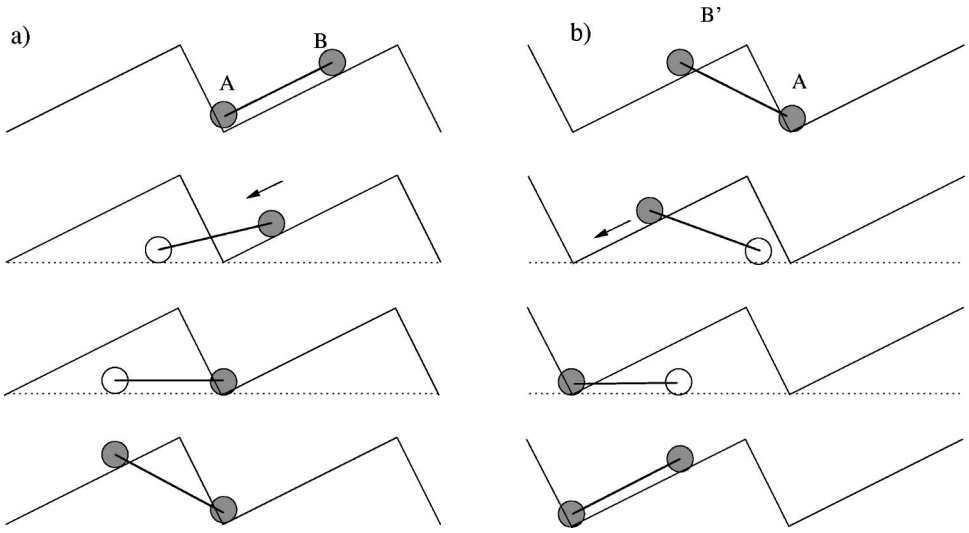

FIG. 4. Driving mechanism for rigidly coupled particles with $l = L/2$.

This driving mechanism can only work if the particle, for which the potential has switched off, can escape from its initial minimum, when it is pushed to the left. This is the case if $l > L_2$.

This driving mechanism also works if z_1 and z_2 fluctuate between two positive values z_a and z_b $(z_a < z_b)$, as long as

$$z_a |f_2| < z_b |f_1|. \tag{25}$$

Indeed this effect can be seen for very small temperature: Fig. 5 shows the current as a function of z_a, when z_b is constant. For the chosen parameters condition (25) holds for $z_a < 0.5$. For small temperature the current vanishes, if $z_a > 0.5$. For higher temperature there is also a current for $z_a > 0.5$, because there is still driving by diffusion.

2. Other stochastic processes

We have done the same calculations for some other stochastic processes of the class defined by Eqs. (14)–(16), namely, for sums of dichotomous processes and discrete kangaroo processes. In all these cases the results are qualitatively similar. Slightly different results are obtained for asymmetric dichotomous processes.

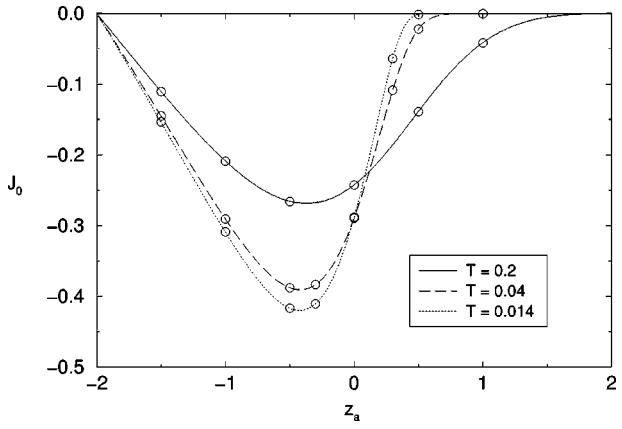

FIG. 5. Driving against a potential well: The current as a function of z_a for constant z_b. For small temperature the current vanishes for $z_a > z_b |f_1|/|f_2|$. $(z_b = 2,\ l = 0.5,\ a = 4,\ \text{and}\ \tau = 0.1)$.

Sums of N dichotomous processes are interesting because in the case of one particle a current reversal for large τ occurs only if N is an even number. For two particles the effective stochastic process in the case $l = 0$ is always an even sum of dichotomous processes. Thus there is a current reversal for all N, provided $z_a < 0$ and $z_a + z_b > 0$. As in the case of a single particle the maximal positive current is smaller for large N. Here the current reversal remains for a larger interval of l. This seems to be due to the current reversal occurring in the one-particle case for $N > 1$. Convergence against the Ornstein-Uhlenbeck process can be seen for $N > 3$. Similar results can be obtained for kangaroo processes with the same stationary probability densities.

We have also studied the case of asymmetric dichotomous processes as an example for a process with different transition times for the transitions $z_a \to z_b$ and $z_b \to z_a$. In this case $\gamma_{0,0} \neq \gamma_{1,1}$. In contrast to the symmetric dichotomous process, for asymmetric dichotomous processes there is a current reversal in the one-particle case [14]. For the case of two particles Fig. 6 shows the current as a function of the correlation time for different values of l. Here a current reversal occurs for all values of l. (For $l = 0$ the negative current which occurs for large τ is very small, and cannot be seen in Fig. 6.) Only the length of the interval of positive current as well as the maximal positive current decrease with increasing l.

B. Order κ^{-1}

1. Dichotomous processes

For dichotomous processes varying between two positive values the correction J_1 to the current is always positive. Thus the current decreases with small oscillations of the particles. If one of the values of the dichotomous process is negative, there is also a change of the sign of J_1 (Fig. 7). This change of sign does not occur at the same value of τ as the current reversal in the case of rigid coupling. Thus in a small region of τ (between the changes of sign of J_0 and J_1)

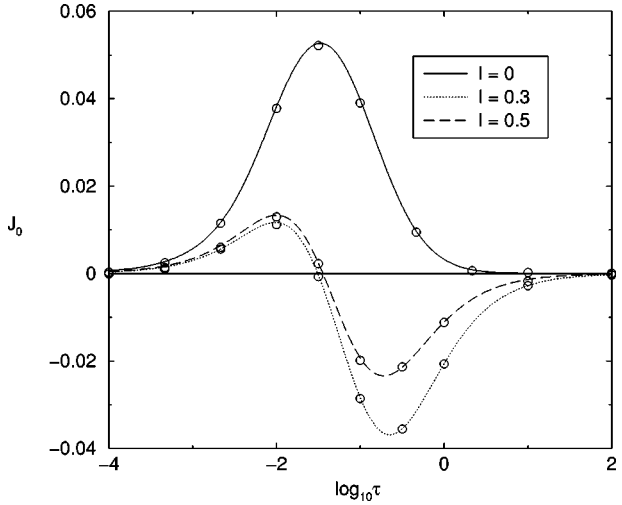

FIG. 6. J_0 for asymmetric dichotomous processes with $z_a=-0.5$, $z_b=1.5$, and a probability $P_a=0.9$ for z_a for different values of l ($a=4$ and $T=0.2$).

the current increases with small oscillations. The behavior of the current as a function of the equilibrium distance is quite complicated. It is shown in Fig. 8.

2. Other stochastic processes

As in the order κ^0, we obtain qualitatively similar results for other stochastic processes. An interesting observation can be made in the case of asymmetric dichotomous processes: In contrast to the order κ^0, where we have found a current reversal for all values of l, the sign of J_1 changes only for small l. Thus we can distinguish two different regimes: If the sign of J_1 changes (the case of small l), there is only a small interval of correlation times in which the current increases with small oscillations of the particles. For larger l instead, the current increases with small oscillations for all correlation times which are smaller than some critical value (Fig. 9).

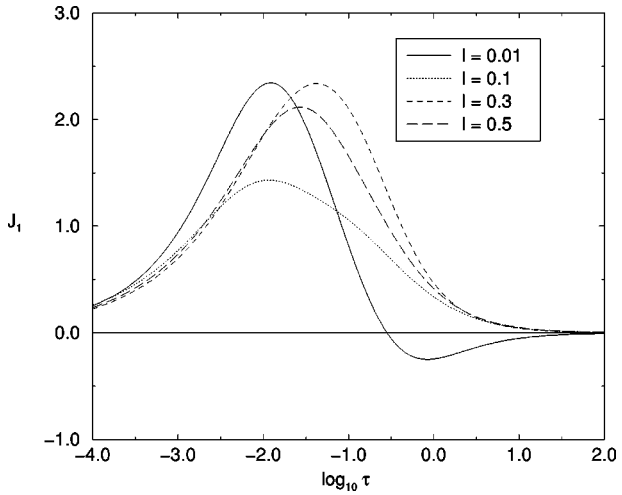

FIG. 7. J_1 for dichotomous processes with $z_a=-0.8$ and $z_b=1.2$ as a function of τ ($T=0.2$ and $a=4$).

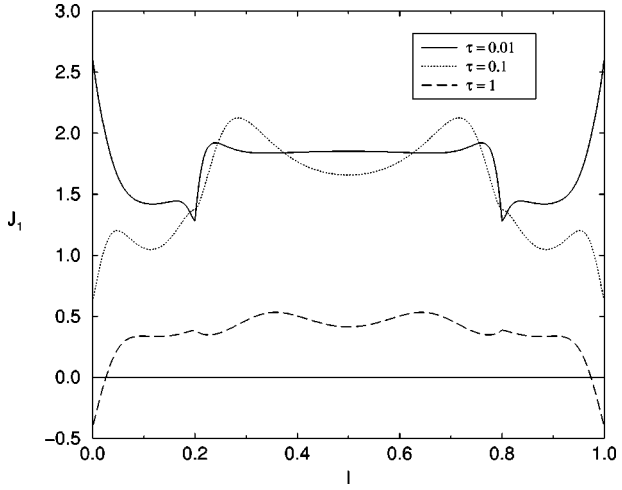

FIG. 8. J_1 for dichotomous processes as a function of l. The parameters are the same as in Fig. 7.

C. Results for finite values of κ

From the results presented so far it is difficult to determine the range of validity of the expansion about the case of rigid coupling. The absolute value of J_1 is in most cases larger by one order of magnitude than that of J_0. This is an indication that the expansion may be valid only for very large κ. However, using the expansion, we can obtain the relative sign of J_0 and J_1. This leads to the interesting qualitative result that small oscillations can increase or decrease the current, depending on the parameters. It may even be possible to reverse the current by changing κ.

Since the absolute value of J_1 is large compared to J_0, one may expect that the series for J in powers of $1/\kappa$ is an asymptotic series. To obtain results for finite κ we performed simulations of the Langevin equations (3) and (4). The simulations yield the stationary current as a function of κ. Results for two different values of l are shown in Figs. 10 and 11.

The figures show that, depending on the other parameters of the system, the current may change the sign as a function of κ. The linear dependence on $1/\kappa$ expected from the expansion can be seen for values of $1/\kappa<10^{-3}$ in our units. For smaller values of κ, the expansion is certainly not valid. On

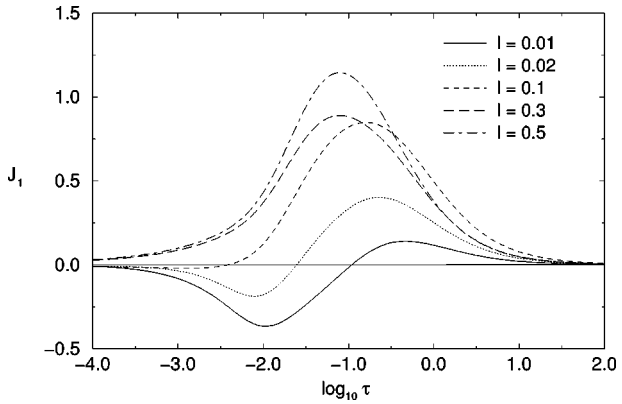

FIG. 9. J_1 for asymmetric dichotomous processes. The parameters are the same as in Fig. 6.

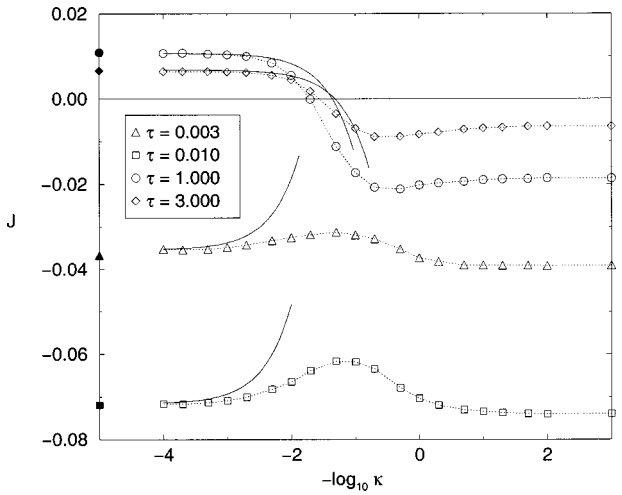

FIG. 10. Simulations for the current as a function of κ for $l=0.01$, $a=4$, and $T=0.2$. $z(t)$ is a symmetric dichotomous process with $z_a=-0.8$ and $z_b=1.2$. Here and in Fig. 11, the results for rigid coupling are inserted at $\kappa=10^5$ (filled symbols); the solid lines indicate the results of the expansion.

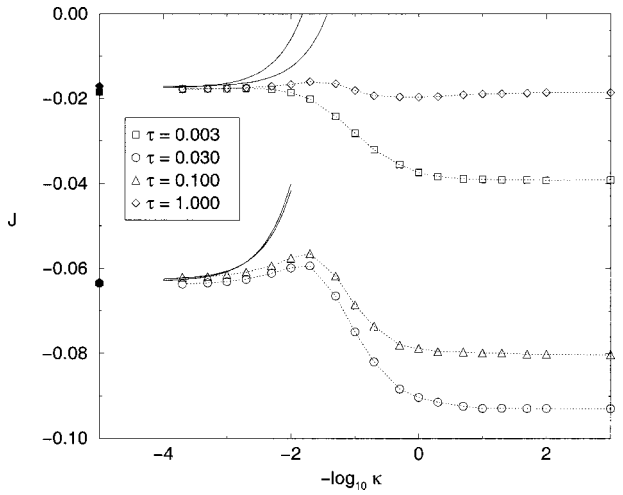

FIG. 11. Simulations for the current as a function of κ for $l=0.3$. The other parameters are the same as in Fig. 10.

the other hand, the order of magnitude of the current remains the same for all values of κ. The results of the expansion and the simulations agree very well for not too small correlation times. Minor agreement for small correlation times is supposed to be due to minor numeric precision in this case.

The current reversal in Fig. 10 can be understood by considering the cases of rigidly coupled particles ($\kappa=\infty$) and uncoupled particles ($\kappa=0$). For small l the case of rigid coupling is essentially equivalent to the one-particle case with a sum of two dichotomous processes. In this case the current is positive for large τ, but negative for small τ. On the other hand if the particles are not coupled at all, the model reduces to two independent simple dichotomous processes and the current remains negative for all values of the correlation time. As the reduction to the single-particle case with a sum of two dichotomous processes is not possible for larger l because of mutual driving, the situation is different in Fig. 11, where no positive current occurs.

VI. SUMMARY AND DISCUSSION

In Sec. V we have presented results for different stochastic processes, and discussed how the current depends on the correlation time τ of the noise, the equilibrium distance l of the particles, and the coupling constant κ. Although the details of the results are rather complex, there are some general features that are common to all the cases studied here.

(1) There is a current reversal if the stochastic parameters fluctuate between positive and negative values, and the sign of the current depends not only on τ but also on l and κ.

(2) There is mutual driving of the particles. This driving mechanism does not need diffusion.

(3) Small oscillations of the particles can increase or decrease the current, depending on the parameters.

As already mentioned in Sec. I, models for noise-induced transport can qualitatively explain some properties of motor proteins: Motion in these models is stochastic, but directed on average, and one obtains a velocity which has the same order of magnitude as the experimentally observed one [6]. As in some cases there is a current reversal in these models, different directions of motion of motor proteins, which have similar structures, can be explained by small differences of the parameters, especially of the friction constant.

It should be emphasized that such a model cannot describe the motion of a motor protein accurately. But it provides a phenomenological description of general aspects based on a rather simple mechanism. The mechanisms occuring in real motor proteins are more complex, and there is a wide diversity of mechanisms adapted to different functions of different motor proteins [15].

In most ratchet models the structure of the motor protein is completely neglected; the protein is treated as a point particle without internal degrees of freedom. Directed motion is due to broken symmetry and broken detailed balance, and structural properties of the motor protein are not essential. Interestingly the driving mechanism changes if two heads are coupled: motion of a single head, modeled by a single particle in a fluctuating potential, is driven by rectified diffusion. In contrast, the results presented in the previous sections, as well as those of Ref. [10], show that coupling two heads leads to a nondiffusive driving mechanism, which provides more efficient driving, as backward steps are less probable. Indeed, similar behavior is found in experiments with one- and two-headed kinesins: the velocity of a single-headed kinesin is smaller by a factor 5, and diffusion stronger by a factor 20, compared to a two-headed kinesin [16]. But though our model has transport properties similar to those observed in kinesin motion, the driving mechanism of a two-headed kinesin is certainly more complex. For example, in contrast to our simple model the kinesin heads are supposed to work in a ''hand-over-hand'' fashion [15].

In this paper we have studied a class of models in which only the amplitude of the potential fluctuates. If the transitions also shift the minimum of the potential, there is a driving mechanism that is similar to the one described here, and does not need diffusion even in the case of one particle [17].

Further refinement of the model would be necessary to

describe motor proteins more realistically. For example the transitions have to occur only at discrete points, the active sites, to obtain qualitatively correct results for the velocity as a function of ATP concentration [7]. If we introduce localized transitions in the present model, the stochastic parameters z_1 and z_2 will no longer be uncorrelated. Though correlations between the two heads of a real motor protein may depend on particular structural properties of the protein, it should be interesting to study how these correlations depend on the parameters in this simple model.

At the end let us mention that the model discussed here may also be realized in an artificial ratchet: The problem, that the potential has to fluctuate independently for each particle, can be solved if the particles move on different tracks that are fluctuating independently.

ACKNOWLEDGMENT

We thank Stephan Altmann for helpful discussions on motor proteins.

APPENDIX A: SOME TECHNICAL ASPECTS OF THE METHOD OF SOLUTION

1. Dependence on $\tilde{y}$

The dependence on $\tilde{y}$ of the functions $\rho_s(x,\tilde{y},z_1,z_2)$, $s=0$, $\frac{1}{2}$, and 1, required to average Eq. (8), is given by the expressions,

$$\rho_0(x,\tilde{y},z_1,z_2)=\frac{1}{\sqrt{\pi T}}\exp\left(\frac{-\tilde{y}^2}{T}\right)\overline{\rho}_0(x,z_1,z_2), \quad \text{(A1)}$$

$$\rho_{1/2}=\frac{1}{\sqrt{\pi T}}\exp\left(\frac{-\tilde{y}^2}{T}\right)\left\{\overline{\rho}_{1/2}(x,z_1,z_2)+\frac{1}{T}\left[z_1 f\left(x+\frac{l}{2}\right)-z_2 f\left(x-\frac{l}{2}\right)\right]\tilde{y}\overline{\rho_0}\right\}, \quad \text{(A2)}$$

$$\rho_1=\frac{1}{\sqrt{\pi T}}\exp\left(\frac{-\tilde{y}^2}{T}\right)\left\{\overline{\rho}_1(x,z_1,z_2)+\frac{2\sqrt{\pi T}}{T}\left[\int_0^{\tilde{y}}d\tilde{y}'F\exp\left(\frac{\tilde{y}'^2}{T}\right)-\int_0^{\infty}d\tilde{y}\int_0^{\tilde{y}}d\tilde{y}'F\exp\left(\frac{\tilde{y}'^2}{T}\right)\right]\right\}, \quad \text{(A3)}$$

with

$$F=\left[\frac{z_1}{2}f\left(x+\frac{l}{2}\right)-\frac{z_2}{2}f\left(x-\frac{l}{2}\right)\right]\rho_{1/2}+\tilde{y}\left[\frac{z_1}{2}f'\left(x+\frac{l}{2}\right)+\frac{z_2}{2}f'\left(x-\frac{l}{2}\right)\right]\rho_0. \quad \text{(A4)}$$

2. Recursion relation for the order κ^0

With ansatz (19), the following recursion relation for the coefficients $p_{i,j}(x)$ is obtained:

$$J_0=\frac{\gamma_{0,0}}{2}f_k^{(+)}p_{0,0}+\frac{\gamma_{0,0}}{2}f_k^{(-)}p_{0,0}-\frac{T}{2}p'_{0,0}-\frac{\gamma_{0,1}}{2}f_k^{(+)}p'_{1,0}-\frac{\gamma_{0,1}}{2}f_k^{(-)}p'_{0,1}, \quad \text{(A5)}$$

$$\frac{\gamma_{0,1}}{2}f_k^{(+)}p_{0,0}=\lambda_1 p_{1,0}+\frac{\gamma_{1,1}}{2}f_k^{(+)}p'_{1,0}+\frac{\gamma_{0,0}}{2}f_k^{(-)}p'_{1,0}-\frac{T}{2}p''_{1,0}-\frac{\gamma_{1,2}}{2}f_k^{(+)}p'_{2,0}-\frac{\gamma_{0,1}}{2}f_k^{(-)}p'_{1,1}, \quad \text{(A6)}$$

$$\frac{\gamma_{0,1}}{2}f_k^{(-)}p_{0,0}=\lambda_1 p_{0,1}+\frac{\gamma_{0,0}}{2}f_k^{(+)}p'_{0,1}+\frac{\gamma_{1,1}}{2}f_k^{(-)}p'_{0,1}-\frac{T}{2}p''_{0,1}-\frac{\gamma_{0,1}}{2}f_k^{(+)}p'_{1,1}-\frac{\gamma_{1,2}}{2}f_k^{(-)}p'_{0,2}, \quad \text{(A7)}$$

$$\frac{\gamma_{i-1,i}}{2}f_k^{(+)}p'_{i-1,j}+\frac{\gamma_{j-1,j}}{2}f_k^{(-)}p'_{i,j-1}=(\lambda_i+\lambda_j)p_{i,j}+\frac{\gamma_{i,i}}{2}f_k^{(+)}p'_{i,j}+\frac{\gamma_{j,j}}{2}f_k^{(-)}p'_{i,j}-\frac{T}{2}p''_{i,j}-\frac{\gamma_{i,i+1}}{2}f_k^{(+)}p'_{i+1,j}-\frac{\gamma_{j,j+1}}{2}f_k^{(-)}p'_{i,j+1}. \quad \text{(A8)}$$

This recursion relation is not tridiagonal as in the case of a single particle [14], but the same methods of solution can be applied.

3. Method for the order κ^{-1}

In this section and in Appendix A 4, we explain the method of solution for the order κ^{-1}, which involves some more technical considerations. Using the same ansatz as for the order κ^0,

$$\rho_1(x,z_1,z_2)=h_{0,0}(x)q(z_1)q(z_2)+\sum_{i,j}(-1)^{i+j}h'_{i,j}(x)\phi_i(z_1)\phi_j(z_2), \quad \text{(A9)}$$

we obtain a recursion relation of the following type:

$$(\lambda_i+\lambda_j)h_{i,j}+\frac{\gamma_{i,i}}{2}f^{(+)}(x)h'_{i,j}+\frac{\gamma_{j,j}}{2}f^{(-)}(x)h'_{i,j}-\frac{T}{2}h''_{i,j}-\frac{\gamma_{i-1,i}}{2}f^{(+)}(x)h'_{i-1,j}-\frac{\gamma_{j-1,j}}{2}f^{(-)}(x)h'_{i,j-1}-\frac{\gamma_{i,i+1}}{2}f^{(+)}(x)h'_{i+1,j}$$
$$-\frac{\gamma_{j,j+1}}{2}f^{(-)}(x)h'_{i,j+1}=-\frac{Tf^{(+)\prime\prime}(x)}{8}(\gamma_{i,i}p'_{i,j}+\gamma_{i-1,i}p'_{i-1,j}+\gamma_{i+1,i}p'_{i+1,j})-\frac{Tf^{(-)\prime\prime}(x)}{8}(\gamma_{j,j}p'_{i,j}+\gamma_{j_1,j}p'_{i,j-1}$$
$$+\gamma_{j+1,j}p'_{i,j+1})-\frac{f^{(+)}(x)f^{(+)\prime}(x)}{4}[(\gamma_{i,i}^2+\gamma_{i-1,i}^2+\gamma_{i,i+1}^2)p'_{i,j}+\gamma_{i-1,i}\gamma_{i-2,i-1}p'_{i-2,j}-\gamma_{i-1,i}(\gamma_{i,i}+\gamma_{i-1,i-1})p'_{i-1,j}$$
$$-\gamma_{i,i+1}(\gamma_{i,i}+\gamma_{i+1,i+1})p'_{i+1,j}+\gamma_{i,i+1}\gamma_{i+1,i+2}p'_{i+2,j}]-\frac{f^{(-)}(x)f^{(-)\prime}(x)}{4}[(\gamma_{j,j}^2+\gamma_{j-1,j}^2+\gamma_{j,j+1}^2)p'_{i,j}$$
$$+\gamma_{j-1,j}\gamma_{j-2,j-1}p'_{i-2,j}-\gamma_{j-1,j}(\gamma_{j,j}+\gamma_{j-1,j-1})p'_{i-1,j}-\gamma_{j,j+1}(\gamma_{j,j}+\gamma_{j+1,j+1})p'_{i+1,j}+\gamma_{j,j+1}\gamma_{j+1,j+2}p'_{i+2,j}]$$
$$+\frac{1}{4}[f^{(+)}(x)f^{(-)\prime}(x)+f^{(-)}(x)f^{(+)\prime}(x)](\gamma_{i,i}\gamma_{j,j}p'_{i,j}-\gamma_{i-1,i}\gamma_{j,j}p'_{i-1,j}-\gamma_{i,i+1}\gamma_{j,j}p'_{i+1,j}-\gamma_{i,i}\gamma_{j-1,j}p'_{i,j-1}$$
$$+\gamma_{i-1,i}\gamma_{j-1,j}p'_{i-1,j-1}+\gamma_{i,i+1}\gamma_{j-1,j}p'_{i+1,j-1}-\gamma_{i,i}\gamma_{j,j+1}p'_{i,j+1}+\gamma_{i-1,i}\gamma_{j,j+1}p'_{i-1,j+1}+\gamma_{i,i+1}\gamma_{j,j+1}p'_{i+1,j+1}). \tag{A10}$$

The difference to the order κ^0 is that here we have additional inhomogeneities. But in the case of a piecewise linear potential the derivatives of the forces are δ and δ' functions; thus the inhomogeneities are zero in the intervals I_k, so that in these intervals we have a recursion relation of the same type as in the order κ^0. The solution for $h_{0,0}(x)$ and $h'_{i,j}(x)$ thus consists of a piecewise continuous part and a sum of δ functions:

$$h_{0,0}(x)=h_{0,0}^{(s)}(x)+\sum_{k=1}^{K}U_{0,0,k}\delta(x-x_k) \tag{A11}$$

$$h'_{0,0}(x)=h'^{(s)}_{0,0}(x)+\sum_{k=1}^{K}V_{0,0,k}\delta(x-x_k)+\sum_{k=1}^{K}U_{0,0,k}\delta'(x-x_k) \tag{A12}$$

$$h_{i,j}(x)=h_{i,j}^{(s)}(x),\quad i+j>0 \tag{A13}$$

$$h'_{i,j}(x)=h'^{(s)}_{i,j}(x)+\sum_{k=1}^{K}U_{i,j,k}\delta(x-x_k) \tag{A14}$$

$$h''_{i,j}(x)=h''^{(s)}_{i,j}(x)+\sum_{k=1}^{K}V_{i,j,k}\delta(x-x_k)+\sum_{k=1}^{K}U_{i,j,k}\delta'(x-x_k). \tag{A15}$$

The piecewise continuous parts are calculated the same way as in the order κ^0. The only difference is that here we have constants $\tilde{b}_{i,j,k}$ containing J_1 instead of $b_{i,j,k}$:

$$h_{0,0}^{(s)}(x)=\sum_{r=1}^{2(N+1)^2-1}\tilde{c}_{r,k}a_{0,0,k}^{(r)}\alpha_k^{(r)}\exp(\alpha_k^{(r)}x)+\tilde{b}_{0,0,k}, \tag{A16}$$

$$h_{i,j}^{(s)}(x)=\sum_{r=1}^{2(N+1)^2-1}\tilde{c}_{r,k}a_{i,j,k}^{(r)}\exp(\alpha_k^{(r)}x)+\tilde{b}_{i,j,k}\quad(i+j>0). \tag{A17}$$

We obtain the coefficients $V_{i,k}$, $i\geqslant 0$ and $U_{i,k}$, $i>0$ by differentiating the incontinuities of the piecewise continuous functions $h_0^{(s)}(x)$, $h_i'^{(s)}(x)$ and $h_i^{(s)}(x)$. Thus we have

$$V_{0,0,k}=h_{0,0}^{(s)}(x_k+0)-h_{0,0}^{(s)}(x_k-0), \tag{A18}$$

$$V_{i,j,k}=h'^{(s)}_{i,j}(x_k+0)-h'^{(s)}_{i,j}(x_k-0), \tag{A19}$$

$$U_{i,j,k}=h_{i,j}^{(s)}(x_k+0)-h_{i,j}^{(s)}(x_k-0),\quad i+j>0. \tag{A20}$$

The coefficients $\tilde{c}_{r,k}$ and the current J_1 are calculated by solving a system of conditions for the δ and δ' functions, and the normalization condition for $h_{0,0}(x)$.

4. Conditions for δ and δ' functions

To calculate the coefficients $\tilde{c}_{r,k}$ and the current J_1 we use a system of conditions for the δ and δ' functions. In this section we show how to derive these conditions from the recursion relation (A10).

We introduce the variable $\epsilon=x-x_k$, where x_k is the border of a potential section, and multiply a continuous test function $t(\epsilon)$ to equation (A10). The width of $t(\epsilon)$ about x_k is small, so we consider only one point x_k. Then we integrate the equation over an interval about x_k. Terms of the order of the width of the test function are neglected. After a partial integration of the terms in which δ' occurs, we have to consider two cases. If the test function is odd, $t(0)=0$ and

thus only terms with $t'(0)$ remain. We obtain the following condition:

$$U_{i,j,k}=\tfrac{1}{4}(f_{k+1}^{(+)}-f_k^{(+)})[\gamma_{i,i}p'_{i,j}(x_k)+\gamma_{i-1,i}p'_{i-1,j}(x_k)+\gamma_{i+1,i}p'_{i+1,j}(x_k)]+\tfrac{1}{4}(f_{k+1}^{(-)}-f_k^{(-)})[\gamma_{j,j}p'_{i,j}(x_k)+\gamma_{j-1,j}p'_{i-1,j}(x_k)+\gamma_{j+1,j}p'_{i+1,j}(x_k)]. \quad \text{(A21)}$$

For an even test function things are a bit more complicated, because there are terms where δ functions are multiplied with incontinuities. Terms like

$$\int d\epsilon\, f^{(+)}(x_k+\epsilon)\,\delta(\epsilon)t(\epsilon) \quad \text{(A22)}$$

are defined as the limits that we obtain if we replace the δ function by an even function with a finite width, integrate, and then let the width go to zero. Thus for the integral not to be zero, $f^{(+)}$ must be an even function, so we replace $f^{(+)}(x_k+\epsilon)$ by

$$\tfrac{1}{2}[f^{(+)}(x_k+\epsilon)+f^{(+)}(x_k-\epsilon)]. \quad \text{(A23)}$$

Proceeding in this way we obtain integrals that are all well defined:

$$\int d\epsilon\, f^{(+)}(x_k+\epsilon)\,\delta(\epsilon)t(\epsilon) = \tfrac{1}{2}[f^{(+)}(x_k+0)+f^{(+)}(x_k-0)]t(0). \quad \text{(A24)}$$

For an even test function terms containing $t'(0)$ vanish, and we obtain a lengthy condition. Using Eqs. (A18)–(A20) a system of equations results, which together with the normalization condition allows us to calculate the coefficients $\tilde{c}_{r,k}$ and the current J_1.

APPENDIX B: MODEL WITH STOCHASTIC FORCES

We have done the same calculations for a model, in which the multiplicative potential fluctuations are replaced by additive stochastic forces. In this model the Langevin equations are

$$\dot{x}_1=f(x_1)+z_1(t)-\tfrac{1}{2}\kappa(x_1-x_2-l)+\sqrt{2T}\xi_1(t), \quad \text{(B1)}$$

$$\dot{x}_2=f(x_2)+z_2(t)+\tfrac{1}{2}\kappa(x_1-x_2-l)+\sqrt{2T}\xi_2(t). \quad \text{(B2)}$$

As opposed to the model with multiplicative fluctuations, here we take only processes with $q(z_i)=q(-z_i)$, so that on average there is no directed force. The calculations described above can be done analogously for this model. In addition, here we can define an effective stochastic force $z=z_1+z_2$. The Fokker-Planck equation in the case of rigid coupling is then equivalent to a Fokker-Planck equation for a particle moving in a potential $V(x-l/2)+V(x+l/2)$ under the influence of the effective stochastic force z. So the results for two rigidly coupled particles are equivalent to results for one particle. If z_1 and z_2 are dichotomous processes or sums of dichotomous processes, the effective stochastic force is always an even sum of dichotomous processes, thus there is always a current reversal.

In the model with multiplicative fluctuations an effective stochastic process $z=z_1+z_2$ can only be defined in the case $l=0$, so that we obtain a Fokker-Planck equation for a particle moving in a fluctuating potential $V(x)z(t)$. The case $l>0$ cannot be reduced to such a one-particle model. As we have shown above, for $l>0$ a driving mechanism occurs, which is different from the one occurring in the one-particle case.

[1] R.D. Astumian, Science **276**, 917 (1997).
[2] F. Jülicher, A. Ajdari, and J. Prost, Rev. Mod. Phys. **69**, 1269 (1997).
[3] J. Rousselet, L. Salome, A. Ajdari, and J. Prost, Nature (London) **370**, 446 (1994).
[4] L.P. Faucheux, L.S. Bourdieu, P.D. Kaplan, and A.J. Libchaber, Phys. Rev. Lett. **74**, 1504 (1995).
[5] M.O. Magnasco, Phys. Rev. Lett. **71**, 1477 (1993).
[6] R.D. Astumian and M. Bier, Phys. Rev. Lett. **72**, 1766 (1994).
[7] J. Prost, J.-F. Chauwin, L. Peliti, and A. Ajdari, Phys. Rev. Lett. **72**, 2652 (1994).
[8] K. Svoboda, C.F. Schmidt, B.J. Schnapp, and S.M. Block, Nature (London) **365**, 721 (1993).
[9] A.J. Hunt, F. Gittes, and J. Howard, Biophys. J. **67**, 766 (1994).
[10] A. Ajdari, J. Phys. I **4**, 1577 (1994).
[11] I. Derényi and T. Vicsek, Proc. Natl. Acad. Sci. U.S.A. **93**, 6775 (1996).
[12] C.S. Peskin and G. Oster, Biophys. J. **68**, 202s (1995).
[13] T. Duke and S. Leibler, Biophys. J. **71**, 1235 (1996).
[14] A. Mielke, Ann. Phys. (Leipzig) **4**, 476 (1995); **4**, 721 (1995).
[15] R.D. Vale and R.A. Milligan, Science **288**, 88 (2000).
[16] Y. Okada and N. Hirokawa, Science **283**, 1152 (1999).
[17] J.-F. Chauwin, A. Ajdari, and J. Prost, Europhys. Lett. **27**, 421 (1994).